Conference Proceedings 4th ICTB (2022)
https://doi.org/10.24451/6j5j-qw13

ICTB 2021PLUS
4th International Conference on Timber Bridges
Biel/Bienne, Switzerland, 9 -12 May 2022

Evaluating the Efficacy of Ground-Penetrating Radar as an Inspection Tool for Timber Bridges

C. Adam Senalik[1], James P. Wacker, Xiping Wang

Abstract

Interest in using ground penetrating radar (GPR) as an inspection tool for wood and wooden structures has increased over the past two decades. GPR provides rapid scanning tool which can provide continuous subsurface information about the structure without the need for direct contact. It is accepted within the steel and concrete industries as a reliable inspection tool. By adapting the GPR for use on wood and wooden structures, the need for an inspector to learn an entirely unique technology is eliminated. Ideally, those familiar with GPR would only need minor instruction on how GPR can be used for wood inspection and hopefully increase the number of skilled inspectors faster than training with a completely unique technology. GPR inspection of wood has been shown to identify moisture, voids, and interior metal. The question remains as to whether GPR can detect internal decay in the absence of water, such as in the case of a covered bridge after a leaking roof has been repaired. This paper reports on a preliminary study, within a comprehensive multi-year effort to investigate GPR technologies, in which the dielectric orthotropy of wood is used to identify regions of interior decay.

1 Introduction

The use of ground penetrating radar (GPR) for inspection of wooden and wood-based structures has increased in the past two decades [1]. GPR has several desirable traits as an inspection tool: it is fast, non-contact, can locate subsurface defects, and is sensitive to the presence of moisture [2]-[8]. It also has several limitations. Radar wave propagation is affected by several factors including frequency of the radar waves, wood density, temperature, size of the specimen, size of the internal defect, and moisture content. Any one or a combination of these factors may be present during inspection [2], [7]-[9]. Despite complicating factors, the advantages of GPR inspection of wood are seen to outweigh the limitations. GPR is seen to have the potential to provide the same rapid, reliable, and non-destructive evaluations for wooden structures as it does for steel and concrete. Toward this end, the United States Department of Agriculture (USDA), Forest Service (FS), Forest Products Laboratory (FPL), in conjunction with the U.S. Federal Highway Administration (FHWA) initiated a multiphase study aimed at expanding the knowledge of GPR behaviour in wood with the goal of making it a more viable option as an inspection tool [10]-[11].

Early applications of GPR inspection of wood bridges occurred in 2002 in Queensland, Australia [4]-[5]. Researchers examined round wood girders during demolition and found excellent agreement between drilling surveys and defect locations as predicted by GPR. The author proposed an inspection regime which would begin with GPR for an initial assessment. In areas where the GPR results indicated the possibility of decay, other inspection tools like micro-resistance drilling or stress wave timing would be used for focused assessment. Another study examined the effect of a bituminous wear protection layer on the ability of GPR to assess the condition of nail laminated bridge decks [10]. The researcher found great potential to identify internal defects within a wooden structure, but widespread presence of the metal nails reflected GPR waves and masking nearby features within the bridge deck. As a result, the GPR signal was degraded which made feature identification within the deck more difficult.

1.1 Multiphase GPR Study

The overarching study, which the research in this paper is a part, has two phases; Phase 1, the tool selection phase, is complete, and Phase 2, the tool evaluation phase, is ongoing. In Phase 1, several non-destructive evaluation (NDE) tools were used to locate air-filled or wet sawdust-filled voids within laboratory constructed specimens. Inspectors with no knowledge of the internal voids were invited to demonstrate the capabilities of the NDE tools and to report their findings. GPR was selected for further study because it identified the highest number of defects and possessed the highest number of desired characteristics for an

[1] C. Adam Senalik, Research General Engineer, USDA, Forest Service, Forest Products Laboratory, United States of America, christopher.a.senalik@usda.gov

inspection tool [12]. In Phase 2, the sensitivity of GPR to moisture content (MC), temperature (T), and decay was explored. A laboratory study using dimensional lumber with varying MC and T were used to characterize how those variables affected GPR output. The method of specimen selection and fungal inoculation is documented in several publications and will only be briefly repeated here [10], [11], [13]. A total of 96 Douglas fir (*Pseudotsuga menziesii (Mirb)Franco*) specimens measuring 81.3 cm in length were inoculated with a brown rot fungus (*Fomitopsis pinicola (Sw.) P.Karst. (1881)*). The specimens had cross sectional dimensions typical of members used in wooden bridges. These field specimens were inoculated with a brown rot fungus and subsequently exposed to weather conditions in the southern United States that promotes rapid fungal growth. Scientists made regular visits and evaluated the wood specimens using a GPR device, collected MC measurements, and obtained stress wave time-of-flight (ToF) measurements. At 6-month intervals, a subset of 12 specimens were returned to the laboratory for further examination using X-ray computerized tomography (CT) and modified hardness testing at critical internal cross-sections [13].

1.2 Current GPR Research

The study is currently in the final portion of Phase 2 in which recorded wave characteristics from GPR are associated with internal decay. From previous studies mentioned above, it is known that GPR can identify moisture pockets and voids that are often associated with decay; however, the ability of GPR to identify decay itself, in the absence of moisture or voids, has not been established. Four fungal inoculated specimens (two glulam beams and two sawn timbers) were collected from the field exposure test site in the Harrison Experimental Forest, near Saucier, Mississippi, United States. This site is characterized as a high fungal decay hazard zone [14]. was chosen as the year-round temperature and humidity promote fungal growth. The middle 51-cm were covered with rigid corrugated plastic which prevented rainwater from contacting the middle portion of the beam. The desire was to have decay begin at the ends of the specimens and then spread to the middle portion through interior decay. The specimens in this study were exposed for over 3.5 years before being collected from the site and returned to FPL. When the specimens were returned, they were examined using X-ray CT. The CT revealed widespread interior moisture, which was corroborated using GPR. The specimens were placed in a humidity and temperature-controlled conditioning room which holds wood at an equilibrium moisture content (EMC) of 12% for three years. With sufficient time having passed for specimens to equilibrate, GPR was once again used to evaluate the specimens.

In this paper, the ability of ground penetrating radar to identify fungal decay in the absence of moisture or voids is examined. At the time of field data collection, there were no significant fungal voids, so the internal moisture was the primary characteristic visible in the GPR radargrams. As the antenna is moved along the surface of the specimen, the GPR sends transmits and receives a radar wave that travels through the depth of the specimen. The wave is transmitted every 2.5-mm of the antenna travel; the distance is measured by an encoder wheel attached to the antenna housing. The individual waves are then aggregated into a single image of through depth waves signals every 2.5-mm apart resulting in a two-dimensional picture known as a radargram. Effort has been made to associate internal features to characteristics within GPR radargrams [15], [16]. With knowledge of regions of internal decay from the CT scans, unique features of the GPR radargrams in the regions of decay can be used to identify indicators of decay in the absence of moisture [17]. This is useful when examining a structure during a dry season in which moisture content may be low, but decay is present. The objective of this paper is to investigate the potential of a new decay identification method using differences in perceived dielectric constant based upon GPR antenna orientation.

The dielectric constant (DC), also known as relative permittivity, is the ratio of the capacitance of a material to the capacitance of a vacuum. The DC governs the speed of an electromagnetic wave through the material; the square root of the DC equals the ratio of the speed of the wave in vacuum to the speed of the wave through the material. The DC, like many of its characteristics, varies based upon the angle of examination with respect to the grain. The DC parallel to the wood grain is greater than the DC perpendicular to the wood grain [9]. For Douglas-fir at 22.8°C and 12% MC, the DC values are around 2.3 parallel to the grain and 1.8 perpendicular to the grain [18]-[20]. As wood decays, the structure of the wood deteriorates. In a fully decayed piece of wood, there should be no differentiation between the DC parallel and perpendicular to the wood grain. In this paper, the relative change of the DC of the specimens is examined when the antenna is changed from parallel to the grain to perpendicular to the grain. It is hypothesized that in areas of extensive decay, the DC values parallel and perpendicular to the wood should be closer in value than in areas of sound wood.

2 Material and method

Four specimens were examined, each having different cross-sectional dimensions: A47, a six-layer glulam beam (13.0-cm × 22.7-cm); B47, a five-layer glulam beam (13.0-cm × 17.8-cm); C47, a solid sawn timber (8.9-cm × 14.0-cm); and D47, a solid sawn timber (8.9-cm × 18.4-cm). They were exposed to field conditions which promoted fungal growth. After a period 3 years and 10 months the four specimens examined in this study were returned to FPL. Upon return, the specimens were tested using GPR, stress wave ToF, and X-ray CT. The specimens were then placed in a humidity and temperature-controlled room at 22.8°C and 50% relative humidity (RH) for a period of 3 years to reach equilibrium at 12% MC. At 12% EMC, the specimens were once again examined using GPR. The GPR and antenna used in this study were a GSSI SIR® 4000 GPR data acquisition system (Nashua, NH) and a 2000 MHz dipole bowtie antenna (DBA) [21]. The GPR radargrams from the specimens were compared to information gained from GPR spans of undecayed control specimens.

The method explored here uses the relative change of DC parallel to the grain versus perpendicular to the grain as a metric for locating interior decay. GPR radargrams of Douglas-fir control specimens at 22.8°C and 12% MC were used to create a baseline threshold indicative of sound wood. The control specimen was a 5 lamina glulam beams with cross sections of 13.0-cm × 17.8-cm. The threshold was then applied to the decayed specimens. Areas of decay within the specimens were also identified using CT scans [22],[23]. The regions of relative change of the DC are then compared to the decay regions identified using the CT scans to determine if correlation exists.

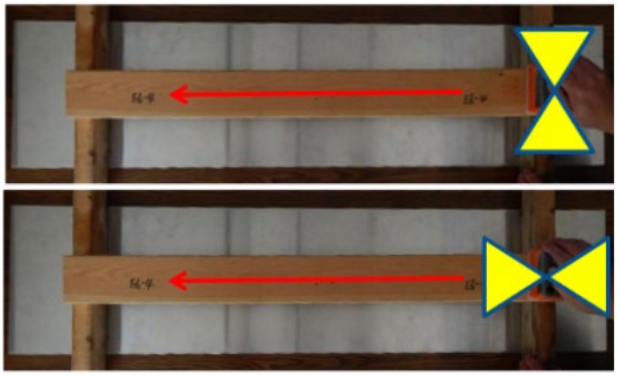

Figure 1: GPR scanning with dipole bowtie antenna, shown here in yellow, oriented perpendicular and parallel to wood grain. In the top (bottom) picture, the antenna is oriented perpendicular (parallel) to the wood grain and generates a field that is parallel (perpendicular) wood grain.

Figure 1 demonstrates the scanning process. The dipole bowtie antenna (DBA) was oriented either parallel to the wood grain or perpendicular to the wood grain. Please note, when the DBA was oriented perpendicular to the wood grain (DBA_{perp}), it generated a field that is parallel to the wood grain. Conversely, when the DBA was parallel (DBA_{para}) to the wood grain, it generated a field that was perpendicular to the wood grain. Therefore, when the DBA was oriented perpendicular (parallel) to the wood grain, it was used to examine the DC of wood parallel (perpendicular) to the wood grain. A thin aluminium sheet was placed under the beam to create a strong reflective boundary at the far side of the specimen. Figure 1 shows supports between the specimen and the aluminium sheet. The supports were not used when scanning the four specimens in this paper.

3 Results

Figure 2a shows the radargram generated using DBA_{perp} for specimen A47. Figure 2b shows the radargram generated using DBA_{para} on A47. In both Figure 2a and Figure 2b, there are notable distortions starting at 63-cm. A metal identification tag was placed on the top of each specimen; the metal tag causes the visible distortion. The dashed line represents the side of the specimen opposite of DBA. In both figures, the double arrow line shows the location of lowest DC of the scan which was used for normalization. For the normalization process, the all values along the dashed line were divided by the average DC value within ±25-mm of the highest DC value.

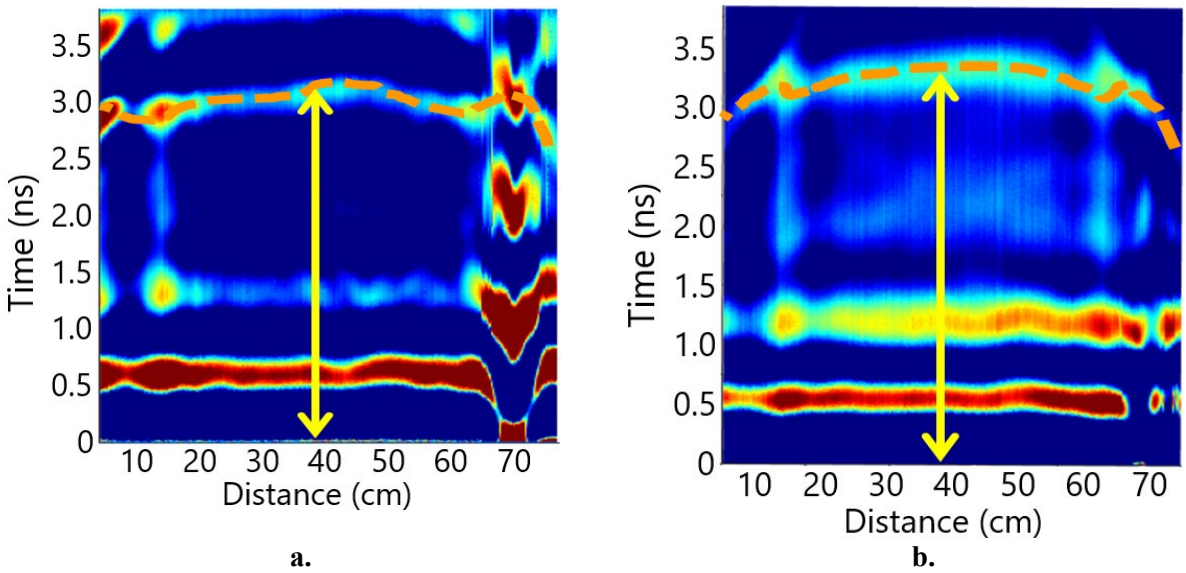

Figure 2: GPR radargram of Specimen A47 with dipole bowtie antenna (DBA). The doubled ended arrow represents the location of the beam used for normalization of the DC. a) DBA oriented perpendicular to wood grain. b) DBA oriented parallel to wood grain.

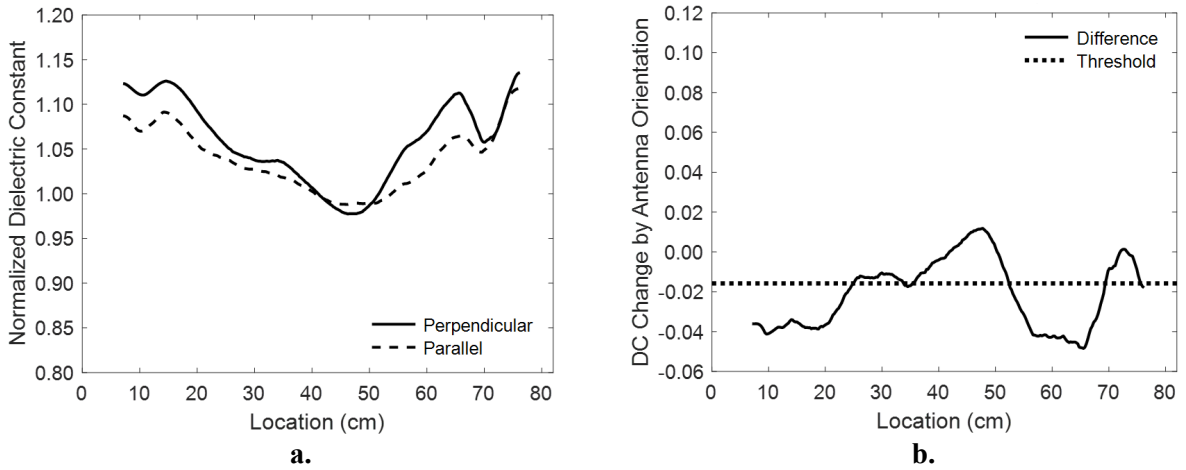

Figure 3: Locating decayed regions in specimen A47. a) Normalized DC along the length with the DBA oriented perpendicular and parallel to the grain. b) Difference in normalized DC for A47 with DBA oriented perpendicular and parallel to the wood grain. The control specimen decay line threshold (Figure 4b) is shown as a dotted line.

Figure 3a shows the normalized DC for the locations along A47. It is at this point the data from the control specimen is introduced. In Figure 4a, the normalized DC along the control specimen generated using DBA_{perp} and DBA_{para} is shown. The two curves tightly overlap. The difference between the values along the curve (perpendicular values minus parallel values) for the control specimen is shown in Figure 4b. The lowest observed value was -0.016 and was treated as the threshold for sound wood. The highest observed value was +0.013. This value was recorded for potential future work to establish an entire range of sound wood values. Figure 3b shows the difference in normalized DC along the curve for A47. The threshold line developed using the control specimen is also shown. Areas from 7-cm to 24-cm and from 53-cm to 68-cm were below the sound wood threshold. Above 68-cm the distortion caused by the metal identification tag obscures decay indicators within the cross section.

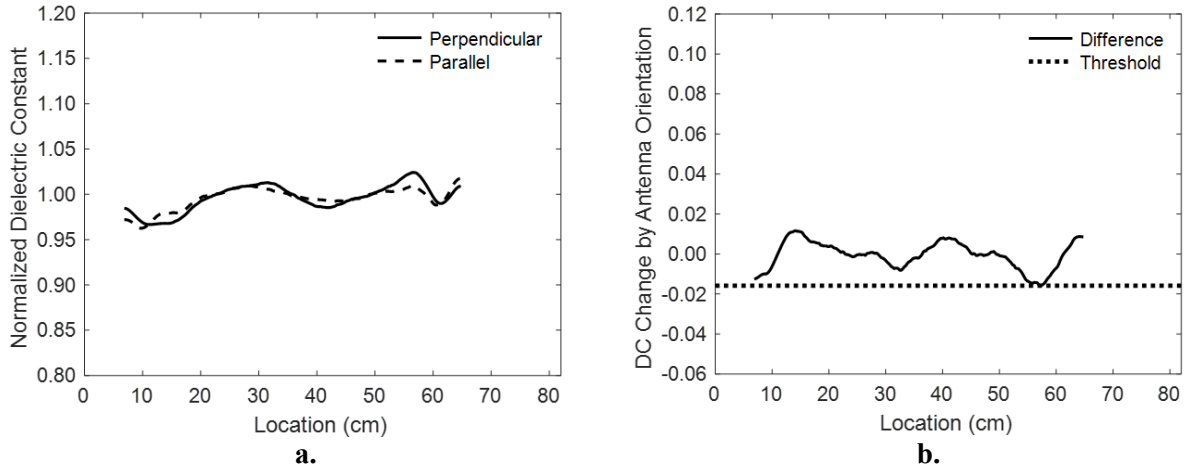

Figure 4: Control specimen threshold determination. a) Normalized DC along the length of the control specimen with the DBA perpendicular and parallel to the grain. b) Difference in normalized DC for control specimen with DBA oriented perpendicular and parallel to the wood grain. The threshold, -0.016, is shown as a dotted line.

Figure 5 shows the difference in normalized DC overlaid across the map in interior decay developed from the CT scan of A4. There was surface decay along the entire top face of A47. During scanning, the DBA was positioned along the top face. The DBA had decreased sensitivity to surface rot at the boundary between DBA housing and the top face of A47. However, the surface rot was easily identified during visual inspection.

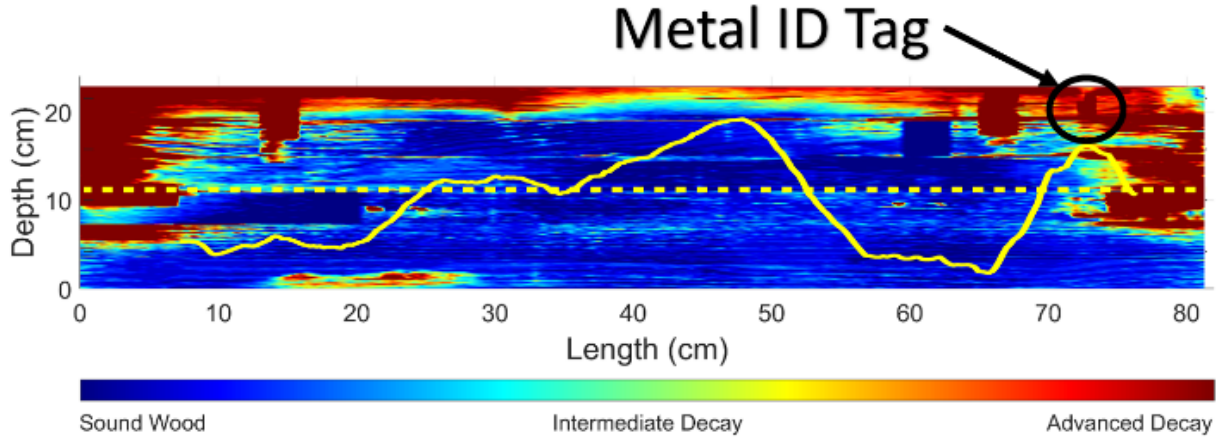

Figure 5: Difference in normalized DC for Specimen A47 with DBA oriented perpendicular and parallel to the wood grain overlaid on a map of decay regions for Specimen A47. Blue regions are sound wood and red regions are areas of advanced decay. The metal ID tag masks underlying decay

Figure 6 shows the normalized DC difference plots for all four specimens. Figure 6a shows A47 from Figure 3b. Figure 6b shows the normalized DC difference plot for specimen B47. The end opposite of the metal identification tag shows clear signs of decay. Like A47, the B47 metal identification tag masked decay beneath the tag. Throughout Phase 2, sawn timbers showed greater decay resistance than the glulam specimens. This resistance has been demonstrated by the decay resistance estimated from CT scans and ToF measurements of stress waves. The resistance was evident in the method examined here. Figure 6c shows the normalized DC difference plot for specimen C47. Two regions dipped below the threshold, at 15-cm and between 60-cm and 72-cm. The region at 15-cm corresponds to the fungal cavity where the specimen was inoculated with brown rot fungus. The region between 60-cm and 72-cm also surrounded a fungal cavity. Figure 6d shows the normalized DC difference plot for specimen D47. The method showed no decay within D47, which was supported by both the CT scan; however, the two fungal dips in the plot correspond to the location of the fungal cavities in D47.

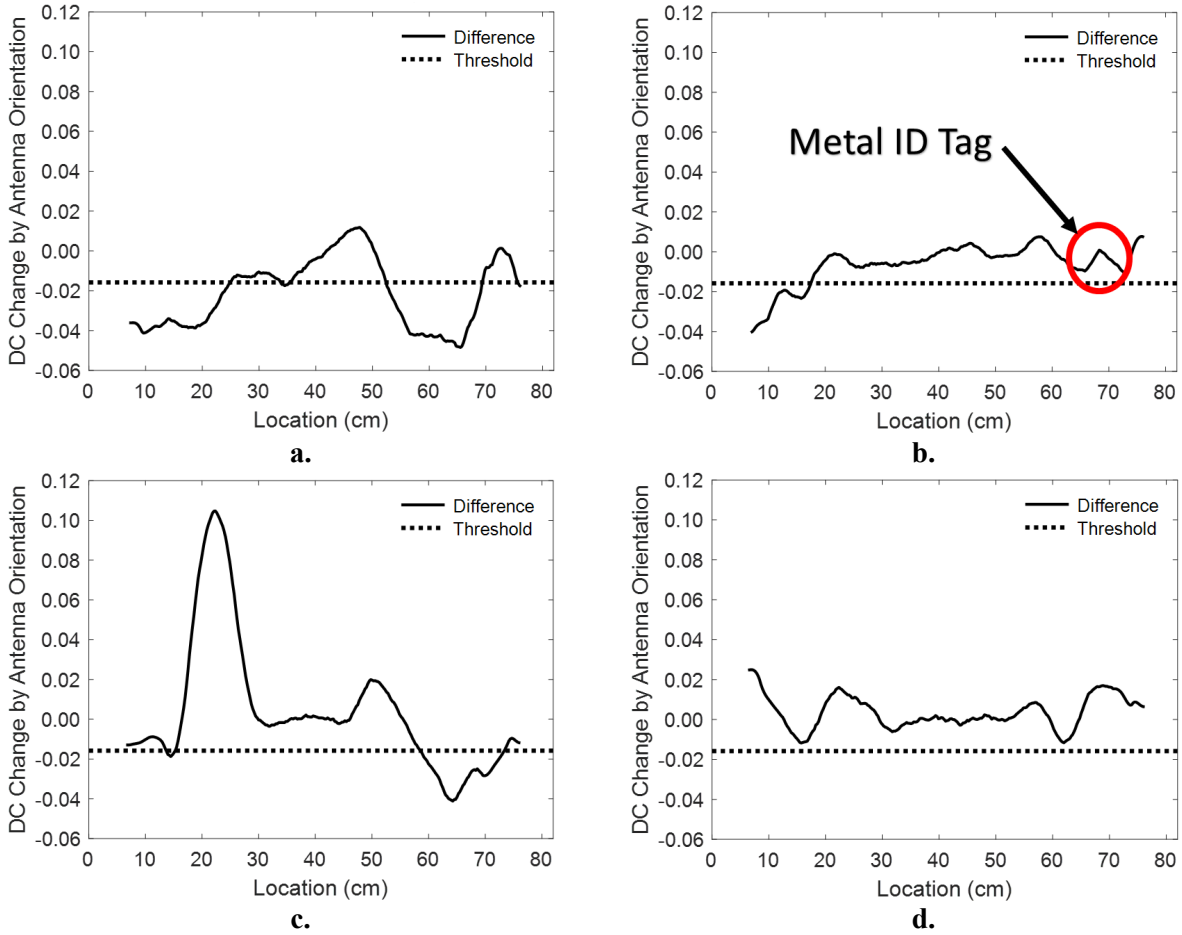

Figure 6: Difference in normalized DC for specimens with DBA oriented perpendicular and parallel to the wood grain. The threshold, -0.016, from Figure 4b is shown as a dotted line. a) A47 as shown in Figure 3b. b) B47. The metal ID tag masks underlying decay. c) C47. Sawn timber specimens have exhibited greater resistance to the brown rot. While the metal ID tag somewhat masks the underlying decay, it still shows the end decay. d) D47. Sawn timber specimens have exhibited greater resistance to the brown rot.

4 Conclusions

This study shows that internal decay may be detected by examining changes in the dielectric constant parallel and perpendicular to the wood grain as measured using a commercially available GPR unit and antenna. A difference in the normalized DC perpendicular to the wood grain minus the normalized DC parallel to the wood grain -0.016 was established as a threshold for sound wood using a control specimen. Good agreement was found between the regions below the threshold for glulam specimen A47 and B47. The sawn timber specimens C47 and D47 showed greater resistance to decay, but C47 exhibited the same differentiation in normalized DC in areas of decay A47 and B47. D47 showed no significant signs of decay in either the CT scan or normalized difference in DC values. The field scanning is rapid using GPR and the steps necessary to perform the procedure are easy to program into any number of computational software packages. The areas of advanced decay predicted by the DC orthotropy model matched the CT scan when only wood was in the region of scanning. The presence of the metal ID tags masked underlying decay. Further work on reducing the distortion caused by interior metal is necessary. The sample examined in this paper represent a small portion of the 96 specimens used in Phase 2. Early promise justifies expanding the number of examined specimens.

Acknowledgements

This study is part of the Research, Technology, and Education portion of the National Historic Covered Bridge Preservation (NHCBP) Program administered by the United States Department of Transportation, Federal Highway Administration. The NHCBP program includes preservation, rehabilitation, and

restoration of covered bridges that are listed or are eligible for listing on the National Register of Historic places; research for better means of restoring and protecting these bridges; development of educational aids; and technology transfer to disseminate information on covered bridges to preserve the Nation's cultural heritage.

References

[1] Rodrigues, Brunela Pollastrelli; Senalik, Christopher Adam; Wu, Xi; Wacker, James. 2021. Use of Ground Penetrating Radar in the Evaluation of Wood Structures: A Review. Forests. 12(4): 492. https://doi.org/10.3390/f12040492.

[2] Mai, T.C.; Razafindratsima, S.; Sbartaï, Z.M.; Demontoux, F.; Bos, F. Non-destructive evaluation of moisture content of wood material at GPR frequency. Constr. Build. Mater. 2015, 77, 213–217.

[3] Cassidy, N.J. Electrical and Magnetic Properties of Rocks, Soils and Fluids. In Ground Penetrating Radar Theory and Applications; Elsevier: Amsterdam, The Netherlands, 2009; pp. 41–72.

[4] Muller, W. Trial of ground penetrating radar to locate defects in timber bridge girders. In Proceedings of the Riding the Wave to Sustainability: IPWEAQ 2002 State Conference, Nossa Lakes, Queensland, Australia, 6–10 October 2002.

[5] Müller, W. Timber girder inspection using ground penetrating radar. Insight Non Destr. Test. Cond. Monit. 2003, 45, 809–812, doi:10.1784/insi.45.12.809.52990.

[6] Rodríguez Abad, I.; Martínez Sala, R.; García-García, F.; Capuz Lladró, R.; Diez Barra, R. A non-destructive method for the evaluation of density and moisture content. In Proceedings of the 12th International Conference on Ground Penetrating Radar, Birmingham, UK, 16–19 June 2008.

[7] Hans, G.; Redman, D.; Leblon, B.; Nader, J.; La Rocque, A. Determination of log moisture content using early-time ground penetrating radar signal. Wood Mater. Sci. Eng. 2015, 10, 112–129.

[8] Hans, G.; Redman, D.; Leblon, B.; Nader, J.; La Rocque, A. Determination of log moisture content using ground penetrating radar (GPR). Part 1. Partial least squares (PLS) method. Holzforschung 2015, 69, 1117–1123.

[9] Torgovnikov, G.I. Dielectric Properties of Wood and Wood-Based Materials; Springer-Verlag Berlin Heidelberg 1993.

[10] Brashaw, B.K. Inspection of Timber Bridge Longitudinal Decks with Ground Penetrating Radar. Ph.D. Thesis, Mississippi State University, Starkville, MS, 39762 USA, December 2014.

[11] Senalik, C.A.; Wacker, J.P.; Wang, X.; Jalinoos, F. 2016. Assessing the Ability of Ground-Penetrating Radar to Detect Fungal Decay in Douglas-Fir Beams. In: 25th ASNT Research Symposium: Summaries and Abstracts. Paper presented at 25th Research Symposium, New Orleans (110-116). Columbus, OH: American Society for Non-destructive Testing, Inc. 7 p.

[12] Wacker, James P.; Senalik, C. Adam; Wang, Xiping; Jalinoos, Frank. 2016. Effectiveness of several NDE technologies in detecting moisture pockets and artificial defects in sawn timber and glulam. In: World Conference on Timer Engineering, WCTE 2016. 22-25 August 2016; Vienna, Austria. 7 pp.

[13] Senalik, C. Adam; Wacker, James P.; Wang, Xiping; Rodrigues, Brunella Pollastrelli; Jalinoos, Frank. 2017. Assessing ability of ground-penetrating radar to detect internal moisture and fungal decay in Douglas-fir beams. In: Wang, X.; Senalik, C.A.; Ross, R.J., eds. Proceedings, 20th international non-destructive testing and evaluation of wood symposium. General Technical Report. FPL-GTR-249. Madison, WI: U.S. Department of Agriculture, Forest Service, Forest Products Laboratory: 286-300.

[14] Scheffer, T.C. 1971. A climate index for estimating potential for decay in wood structures above ground. Forest Products Journal. 21(10): 25–31.

[15] Wu, XI; Senalik, Christopher Adam; Wacker, James; Wang, Xiping; Li, Guanghui. 2019. Using ground penetrating radar to classify features within structural timbers. In: Wang, X.; Sauter, U.H.; Ross, R.J., eds. 2019. Proceedings: 21st International Nondestructive Testing and Evaluation of Wood Symposium. General Technical Report FPL-GTR-272. Madison, WI: U.S. Department of Agriculture, Forest Service, Forest Products Laboratory. pp 502-510.

[16] Wu, Xi; Senalik, Christopher Adam; Wacker, James; Wang, Xiping; Li, Guanghui. 2020. Object detection of ground-penetrating radar signals using empirical mode decomposition and dynamic time warping. Forests. 11(2): 230.

[17] Wu, Xi; Senalik, Christopher Adam; Wacker, James P.; Wang, Xiping; Li, Guanghui. 2020. Ground-penetrating radar investigation of salvaged timber girders from bridges along Route 66 in California. Wood and Fiber Science. 52(1): 73-86. https://doi.org/10.22382/wfs-2020-007.

[18] Wittkopf, J.J.; MacDonald, M.D. 1949. Dielectric Properties of Douglas Fir at High Frequencies. Oregon State Engineering Experiment Station Bulletin 28, July 1949.

[19] Mai, T.C.; Sbartaï, Z.M.; Bos, F. Non-destructive evaluation of wood moisture content using GPR technique—Effect of fiber direction and wood type. In Proceedings of the International Symposium Non-Destructive Testing in Civil Engineering (NDT-CE), Berlin, Germany, 15–17 September 2015.

[20] Rodríguez-Abad, I.; Martínez-Sala, R.; García-García, F.; Capuz-Lladró, R. Non-destructive methodologies for the evaluation of moisture content in sawn timber structures: Ground-penetrating radar and ultrasound techniques. Near Surf. Geophys. 2010, 8, 475–482, doi:10.3997/1873-0604.2010048.

[21] Geophysical Survey Systems, Inc (2014) SIR 4000 manual. Geophysical Survey Systems, Inc., Nashua, NH. https://www.geophysical.com/wp-content/uploads/2017/10/GSSI-SIR4000-Manual.pdf .

[22] Senalik, Christopher Adam; Wacker, James; Wang, Xiping; Wu, Xi. 2019. Identifying incipient decay in Douglas-fir bridge components using x-ray computerized tomography. In: Wang, X.; Sauter, U.H.; Ross, R.J., eds. 2019. Proceedings: 21st International Nondestructive Testing and Evaluation of Wood Symposium. General Technical Report FPL-GTR-272. Madison, WI: U.S. Department of Agriculture, Forest Service, Forest Products Laboratory: 62-70.

[23] Bucur, V. 2003. Nondestructive characterization and imaging of wood. Berlin Heidelberg New York: Springer.